

Enhancing Transient Response of Asymptotic Regulation with Disturbance Onset

Kevin C. Chu and Tsu-Chin Tsao*

Abstract—In incorporating an internal model (IM) to an linear time invariant (LTI) feedback system to achieve asymptotic regulation for exogenous disturbances, limitation in robust stability often hinders the transient response performance, such as the convergence rate and maximum output magnitude, of the LTI closed loop system. When the onset time of the disturbance introduced to the system is known, we formulate a linear time varying (LTV) controller, which exploits this information to improve the transient performance while maintaining the asymptotic regulation and desired robust stability. Simulation and experimental results for asymptotic regulation of a linear motor are presented to demonstrate the improvement of the proposed LTV over LTI controller.

I. INTRODUCTION

The internal model principle [1] has been used to cancel exogenous signal by generating dynamics in the feedback path between the input and output to be regulated. By placing the dynamics of the disturbance within the feedback path, the system is able to achieve asymptotic convergence. Many different implementations and approaches have proposed to satisfy this constraint, such as Internal Model Principle (IMP) [2] and Adaptive Feedforward Compensation (AFC) [3]. These approaches all achieve asymptotic performance, however many of approaches involve time invariant controllers limiting, which have many limitations on their own. If a time-invariant control is implemented in a real setting, it should be constrained by standard robust stability constraints [4]. However because of these robust stability constraints, the these controllers cannot be set to be arbitrarily aggressive to achieve faster convergence rates.

There are many applications in which an exogenous disturbance is known to occur at specific times, such as non-circular cutting and hard disk drives [5], [6]. Sinusoidal disturbance cancellation have been of much interest [7], [8], [9], in hard disk drives because whenever a new seek command to another track is issued, a new Repeatable Runout Error (RRO) must be compensated for due to track offset. If this disturbance is too large, track writing cannot occur. This time onset of disturbance is known correspond with every seek command, however, the magnitude and phase of the disturbance is unknown ahead of time. If a faster disturbance rejection time can occur, the seek time is reduced and more data throughput can be handled. Another common problem in vibration control [10], where an external

sinusoidal may influence the performance of the underlying system, would be improved with faster disturbance rejection. Faster recoveries from disturbances will improve efficiency of any systems. Under time-invariant control applications, the robust controller cannot automatically handle changing dynamics. Intuitively, if the disturbance perturbations are known ahead of time, the information should be used to help improve the convergence performance.

In this paper, we propose a time varying controller based on the disturbance estimator Kalman filter. By augmenting the system's state to incorporate the disturbance dynamics, the sudden change in disturbance dynamics can be modeled as process noise specific to those disturbance states. In doing so, the gains of the Kalman filter automatically adjust and allow for faster learning of those new dynamics allowing for faster convergence, while maintaining long term robust stability.

The remainder of this paper is organized as follows: In Section II, the problem is setup and the control algorithm is described. In Section III, the algorithm is simulated on a modeled plant, and in Section IV, the algorithm is transferred to the real plant on a real time controller. The results are then studied. Section V then concludes the paper.

II. PROBLEM SETUP

Let P be any plant and C be any preselected controller as seen in Figure 1. The plant is perturbed by a disturbance

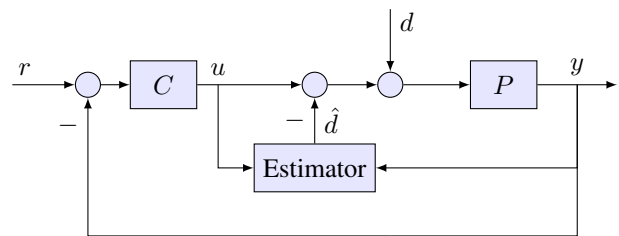


Fig. 1. Plug In Block Diagram for Disturbance Estimator

signal d which contains is composed of sinusoidal signals that can described by

$$d = a(t) + \sum_{i=0}^n \alpha_i(t) \sin(\omega_i t + \phi_i(t)) \quad (1)$$

where a describes a constant disturbance and α , ω and ϕ describe the amplitude, frequency and phase of a respective sinusoidal exogenous disturbance. The magnitude of the disturbance can have sharp transitions at known specific

This work was supported in part by the National Science Foundation under grant no. DMI 0327077 and CMMI 0751621

Kevin C. Chu and Tsu-Chin Tsao are with the Department of Mechanical and Aerospace Engineering, University of California, Los Angeles, California, 90025, USA. kchu@ucla@gmail.com, ttsao@ucla.edu

times. However the value of those exact magnitude and phase change of those changes may not be known ahead of time. It is assumed that both $\alpha(t)$ and $\phi(t)$ have step like transitions during changes, however this method can also handle slowly changing signals.

The goal of the estimator in figure 1 is to estimate d with \hat{d} and cancel it out. The problem is placed in the framework of a Kalman filter [11]. Estimating the state is not the main objective; instead, the goal is to determine the characteristics of the disturbance introduced. As so, the estimator does not need to estimate the state of the controller, but only those of the plant and the disturbance. The pre-designed controller can be non-linear and time-varying since only the control signal u is necessary.

Assume the discrete linear plant P can be described by

$$x(k) = Ax(k-1) + Bu(k-1) + Bd(k-1) + w(k-1) \quad (2)$$

$$y_k = Cx_k + v_k \quad (3)$$

where w_k and v_k are the process noise and measurement noise, respectively.

The plant state is then augmented to model the sinusoidal disturbances as

$$x_{aug} = \begin{bmatrix} x \\ x_d \end{bmatrix} \quad (4)$$

which are modeled by:

$$x_d(k) = A_d x_d(k-1) + w_d(k-1) \quad (5)$$

where A_d is made up of block diagonals containing the internal model, where the first entry describes the constant disturbance.

$$A_d = \begin{bmatrix} 1 & & & & & & & & & & 0 \\ & \begin{bmatrix} 2 \cos(\omega_1) & -1 \\ & 1 & 0 \end{bmatrix} & & & & & & & & \\ & & \ddots & & & & & & & & \\ & & & & \ddots & & & & & & \\ 0 & & & & & & \begin{bmatrix} 2 \cos(\omega_m) & -1 \\ & 1 & 0 \end{bmatrix} & & & & \end{bmatrix} \quad (6)$$

and w_d describes the possibility of drifting of the disturbance. Combining eq. (2), (4) and (5), the overall system yields:

$$x_{aug} = \begin{bmatrix} x(k) \\ x_d(k) \end{bmatrix} = \begin{bmatrix} A & BC_d \\ 0 & A_d \end{bmatrix} \begin{bmatrix} x(k-1) \\ x_d(k-1) \end{bmatrix} \quad (7)$$

where $C_d = [1 \ 0 \ 1 \ 0 \ \dots \ 1 \ 0 \ 1]$ simply describes how the noise is injected from the disturbance states to the plant input. Note that where the disturbance states are independent and uncontrollable.

The filter uses the standard discrete Kalman coefficient updates [12],[13].

$$\begin{aligned} \hat{x}(k|k-1) &= A\hat{x}(k-1) + Bu(k-1) \\ P(k|k-1) &= AP(k-1)A^T + Q(k) \\ L(k) &= P(k|k-1)C^T(CP(k|k-1)C^T + R)^{-1} \\ \hat{x}(k) &= \hat{x}(k|k-1) + L(k)(y(k) - C\hat{x}(k|k-1)) \\ P(k) &= (I - L(k)C)P(k|k-1) \end{aligned}$$

where, P is the error covariance, and L represents the Kalman gain. Note that the process noise covariance $Q(k)$ is able to change with time. Stability and convergence have already been proven within the Kalman Filter framework [14].

A. Q and R Selection

Under standard definitions Q is defined as $Q = E[vv^T]$, however after the state augmentation,

$$Q_{aug} = E \begin{bmatrix} v \\ v_d \end{bmatrix} \begin{bmatrix} v & v_d \end{bmatrix} \quad (8)$$

$$= \begin{bmatrix} Q & 0 \\ 0 & Q_d \end{bmatrix} \quad (9)$$

The original process noise covariance matrix Q and measurement noise covariance matrix R are still determined using standard methods. This paper's main flexibility arises from the ability to tune Q_d to both ensure steady state robust stability and allow for faster convergence to a change in disturbance. We propose that Q_d is chosen to temporarily increase to a large magnitude when the onset of disturbance is pre-known to change, while maintaining a smaller value during the rest of the time. By doing so, the Kalman gains temporarily increase to quickly learn the evolution of the disturbance parameters, and then later return to the original conservative learning gains. The controller provides fast learning, while maintaining long term stability. By putting the disturbance estimation within the Kalman filter framework, this controller affords the designer an stochastically optimal convergence.

B. Selection of Q_d

There are two main circumstances that the process noise covariance matrix Q_d must be chosen:

- 1) Steady State Performance $Q_{d,ss}$
- 2) Onset disturbance transitions $Q_{d,trans}$

Under nominal conditions, as long as Q_d remains positive definite, the overall system is guaranteed to be stable. However, under robust stability constraints, the steady state $Q_{d,ss}$ are constrained in magnitude. By increasing $Q_{d,ss}$ arbitrarily large, the complementary sensitivity can fall outside of acceptable bounds. Unfortunately as shown in [15], it is shown there are no bounds that can be known ahead of time; only the designed controller can be checked to be robustly stable. In practice, the limits of Q_d can be checked against an uncertainty bound W_r , or tuned on the actual system to achieve acceptable performance.

On the other hand, the lower bound of $Q_{d,ss}$ can be arbitrarily small. Another benefit is as $Q \rightarrow 0$ the loop gain of the system returns to the pre-designed controller, which is assumed to already be within acceptable bounds. If $Q_{d,ss} = 0$, the system essentially freezes the disturbance state estimation and maintains a constant disturbance cancellation. This intermittent learning yields similar benefits to [16], but allows for a more formal and straightforward setup. This formulation also allows sinusoidal disturbances instead of only a steady state disturbance cancellation.

During disturbance transitions, $Q_{d,trans}$ should be chosen to accommodate the approximate $E[v_d v_d^T]$, however any small increase in $Q_{d,trans}$ relative to $Q_{d,ss}$ yields larger learning gains for disturbance cancellations.

So under sharp transitions in disturbances, Q_d can be defined as

$$Q_d(k) = \begin{cases} Q_{d,trans} & k \in \mathcal{K} \\ Q_{d,ss} & \text{otherwise} \end{cases} \quad (10)$$

where \mathcal{K} represents the set of times k such that an onset of disturbance transition occurs. It should be of note, if the plant model does not match the real plant, in order to maintain stability these disturbance must be far enough apart in time such that the elevated Kalman gains L can return to normal levels and stabilize the system. Sustained impulses of $Q_{d,trans}$ may have the ability to destabilize the system.

III. SIMULATION AND RESULTS

The algorithm is implemented on a Halbach linear motor described in [17] is shown in Figure 2. The open loop plant was modeled using N4SID and its bode plot can be seen in Figure 3. The open loop system resembles a double

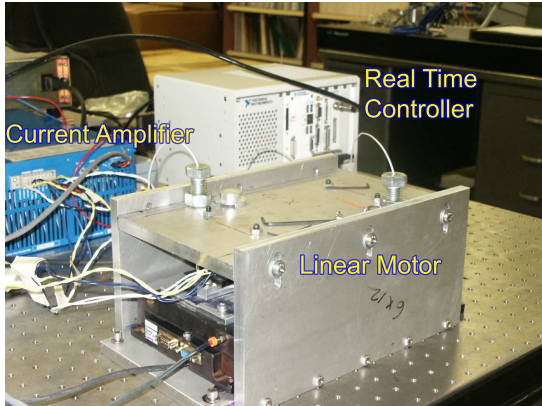


Fig. 2. Linear Motor Setup

integrator. The system has an update rate of 5kHz and is controlled by C using manually tuned PD controller with a goal to maximize the bandwidth. The regulation reference was chosen to show disturbance characteristics. A PD controller did not have to be chosen for its simplicity but also to show the algorithms flexibility to fit within common framework. Due to the fact that the states are already estimated with a Kalman filter, a state feedback controller using LQR [18] can also be easily designed within this scheme.

An artificially generated sinusoidal disturbance at 60Hz of amplitude 0.3 Volts is inserted as d , that intermittently affects the system as seen in Figure 4. The sinusoid abruptly increases in magnitude. The results are similar to any phase change or similar amplitude change. Below the input disturbance graph, Figure 4 shows the onset transitions for Q_d . During the transition times, when the value goes to one, $Q_d = Q_{d,trans}$, and $Q_d = Q_{d,ss}$, when the value goes to zero.

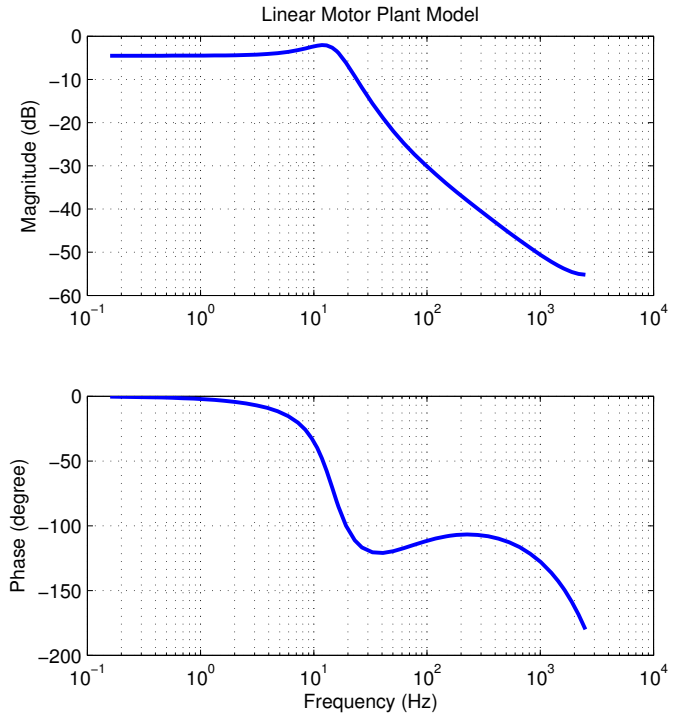


Fig. 3. Bode plot of the linear motor model

For the experiment, both $Q_{d,ss}$ and $Q_{d,trans}$ are chosen to be diagonal matrices multiplied by a scalar. The steady state $Q_{d,ss}$ is chosen to push the performance, nearing robustness bounds. Increasing $Q_{d,ss}$ further caused system instability. The transitional $Q_{d,trans}$ was tuned to be 4 order of magnitudes larger than $Q_{d,ss}$. If instead $Q_d = Q_{d,trans}$ is chosen, the system goes unstable. In these simulations, the time-varying impulsive Q_d , is compared to its steady state counterpart, where $Q_d = Q_{d,ss}$ during the entire simulation.

By implementing a jump in Q at the onset of amplitude changes, we can easily see a jump in the correction gains L of the Kalman filter as seen in Figure 5. It can be noted that these values do *not* change if the two Q_d values remain consistent throughout the experiment. These values can be pre-calculated and put in a look up table to save on the high computational cost of the Kalman filter, reducing the complexity of computation down to a simple time-varying Luenberger Observer. However if either value of $Q_{d,ss}$ or $Q_{d,trans}$ cannot be known ahead of time, the original Kalman implementation must be used. Also for this configuration, the gains all return to steady state bounds within 0.2 seconds. As hoped for, the largest two value changes in L correspond to the sinusoidal disturbance states. The third largest correspond to the steady state gains. The last three, which correspond to the plant states, hardly change at all.

It may be useful to show the sensitivity functions of the control systems with just the PD control, with an observer with $Q = Q_{d,ss}$, and with an aggressive observer with $Q = Q_{d,trans}$. Although in implementation, the values of Q vary with time we allow the Kalman gains steady state

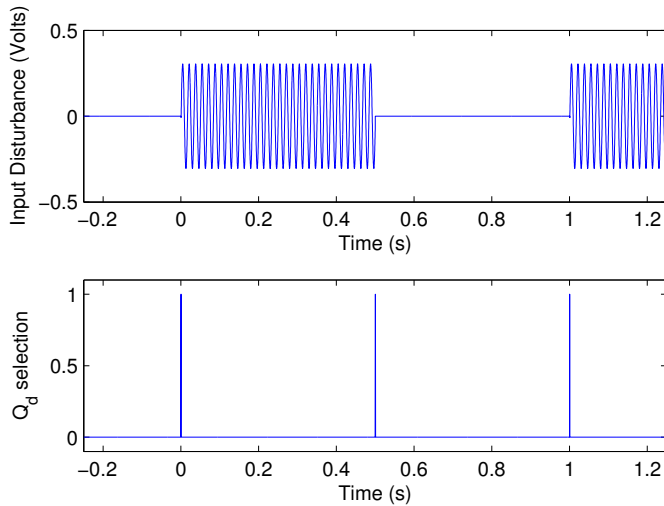


Fig. 4. Intermittent disturbance signal d injected at control input. Also the onset transitional states for $Q_{d,trans}$ are shown in the bottom graph. When the sinusoidal disturbances transition, the decision goes to 1 and $Q_d(k) = Q_{d,trans}$. Otherwise, the decision stays at zero, and $Q_d = Q_{d,ss}$.

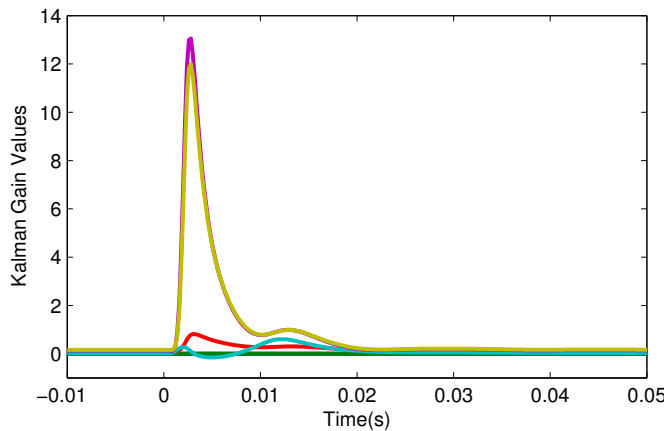


Fig. 5. Evolution of Kalman learning gains L during the transition

to observe the steady state sensitivity and complementary sensitivity functions, as seen in Figure 6. As expected, the PD control has no rejection of any periodic disturbance, while $Q = Q_{d,ss}$ and $Q = Q_{d,trans}$ do. It can also be seen that the $Q = Q_{d,trans}$ has a much faster drop off at $\omega = 0\text{Hz}$ and $\omega = 20\text{Hz}$. It may be concluded that the better choice would always be $Q = Q_{d,trans}$, but if we look at the complementary sensitivity function as seen in Figure 7, we can see that the more aggressive Q causes a much larger gain in the higher frequencies. By having a larger gain, the robust stability of our system can no longer be guaranteed. It should be of note, that $Q_{d,ss}$ can be chosen to be zero which would return both the sensitivity and complementary sensitivity functions back to the original PD control.

Figure 8 shows the simulation results for the estimate of \hat{d} to d . As we can see, by time-varying the Q_d , the disturbance rejection time converges much faster than the non time-varying version. Instead of taking multiple periods to estimate the disturbance, the algorithm begins the estimate

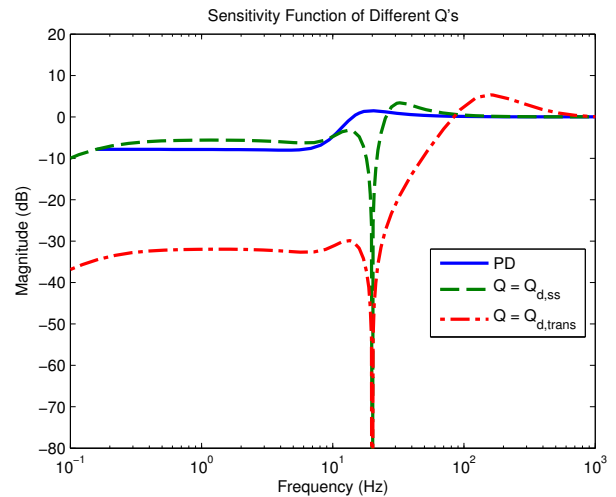


Fig. 6. Steady state sensitivity functions of different choices for Q

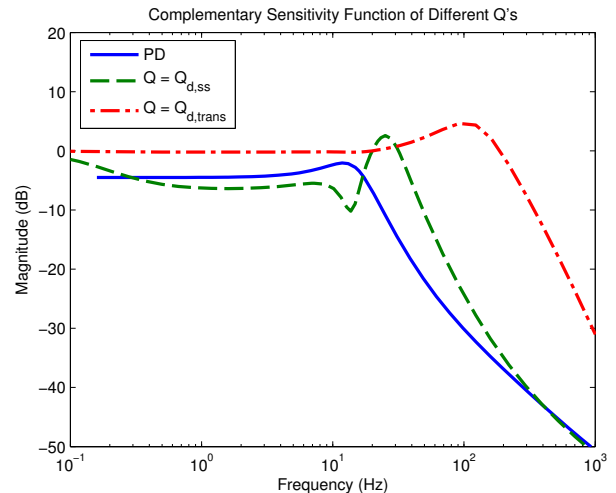


Fig. 7. Steady state complementary sensitivity functions of different choices for Q

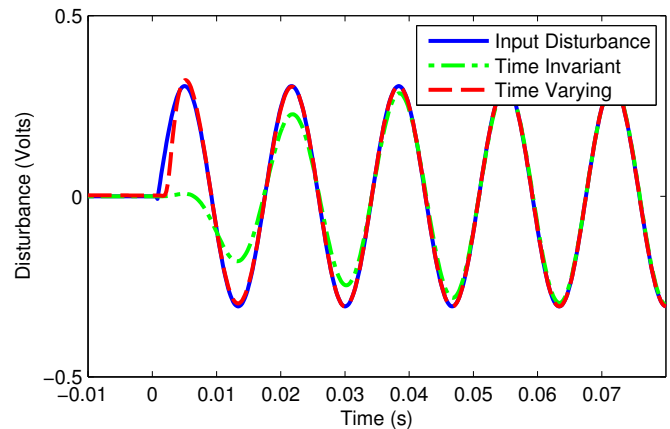


Fig. 8. Simulation: Disturbance estimation on onset of sinusoidal disturbance

the correct magnitude and phase within one cycle.

For the true regulation error y , as seen in Figure 9 the

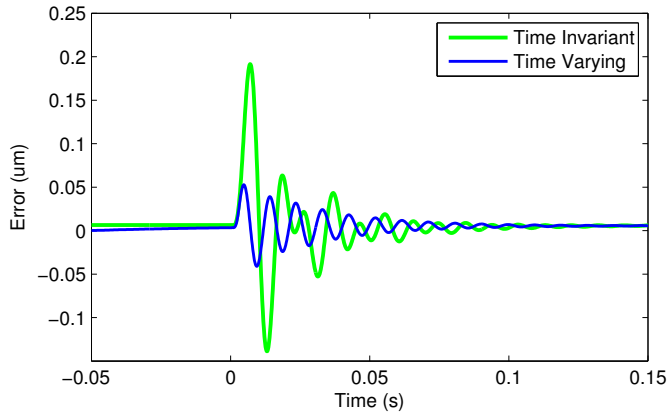


Fig. 9. Simulation: Output error performance due to an onset of sinusoidal disturbance

time it takes the system to correct to the sinusoidal change is greatly reduced for the time-varying case. Regardless of transition, the results are similar. The fall at time $t = 0.5$ seconds in Figure 4, has very similar results to $t = 0$ seconds, and thus is not shown.

Because the disturbance model also can incorporate a constant disturbance, this formulation can also account for steady state error and correct for it. Another benefit, is that it can also improve step jumps in the reference as well. To test this, a constant disturbance is injected at time $t = 0$ with a value of 0.3 volts, as can be seen in Figure 10. Under the

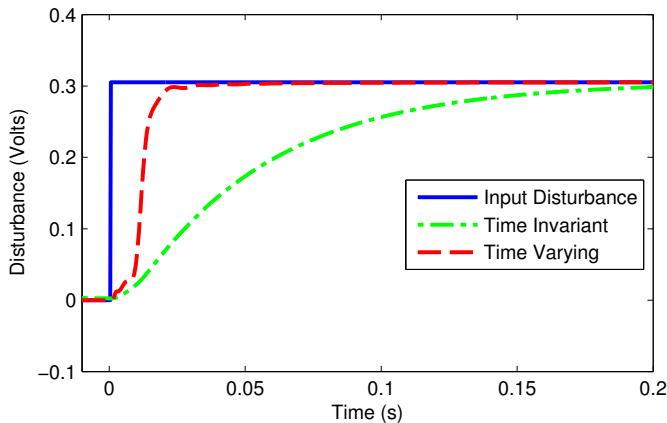


Fig. 10. Simulation: Disturbance estimation on the onset of a constant disturbance

time invariant case, the states take more than 0.2 seconds to accurately estimate this additional disturbance. However, the time varying Q_d achieves the same estimation in a fraction of the time.

IV. EXPERIMENTAL RESULTS

In real implementation, the plant may be slightly perturbed from our model due to modeling errors. Even with modeling errors, Figure 12 still shows the drastic improvement in

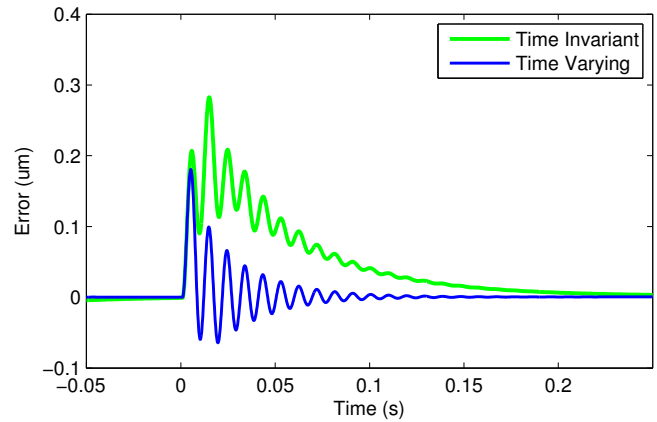


Fig. 11. Simulation: Output error performance due to a constant disturbance onset

estimation convergence time due to an onset of a sinusoidal disturbance. The simulation and experimental results do not match exactly, but the functionality remains the same. The output errors shown in Figure 13 shows a similar

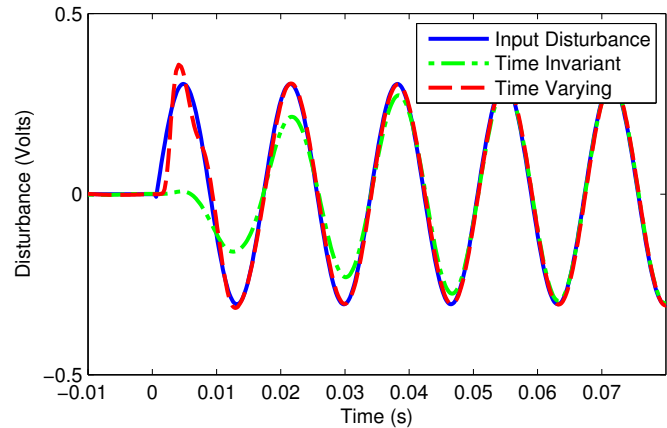


Fig. 12. Experiment: disturbance estimation on the onset of sinusoidal disturbance

convergence rate to that of the disturbance estimation. The maximum perturbation decreases from .2 micrometers to 0.05 micrometers.

Since a constant disturbance is also incorporated in the internal model, the algorithm is also able more quickly estimated steps changes in the error disturbance as seen in Figure 14. However due to the fact that real system encounters a constant disturbance most likely due to the motor amplifier bias, the estimation is offset by about 0.3 volts. Regardless of the sources of constant disturbance, the algorithm is able to estimate the magnitude of the change in much the same way the simulation did. Also, the output errors as seen in Figure 15 converge similarly with the time varying control having a drastically faster convergence rate than the time invariant control. The peak error is also reduced from 1.8 micrometers to 0.8 micrometers.

V. CONCLUSION

By formulating the internal model into a Kalman disturbance estimator and simply adjusting its process noise with respect to time, the algorithm is able to automatically adjust its own gains to learn the changes to the disturbance more quickly with the a priori knowledge of the onset time of the disturbance. With the faster estimation convergence, asymptotic regulation of the output is also achieved at a similar rate. Furthermore, the proposed linear time varying control algorithm is able to quickly return back to the robust steady state LTI controller. The simulation and experimental results have demonstrated that the LTV control was able to drastically reduce both the maximum output and the transient time over those of the LTI control.

REFERENCES

- [1] B. Francis and W. Wonham, "The internal model principle of control theory," *Automatica*, vol. 12, pp. 457–465, Sept. 1976.
- [2] Y. Wang, K. Chu, and T. Tsao, "An analysis and synthesis of internal model principle type controllers," *American Control Conference*, pp. 488–493, 2009.
- [3] M. Bodson, A. Sacks, and P. Khosla, "Harmonic generation in adaptive feedforward cancellation schemes," *IEEE Transactions on Automatic Control*, vol. 39, no. 9, pp. 1939–1944, 1994.
- [4] K. Zhou, J. Doyle, and K. Glover, *Robust and optimal control*. Prentice Hall Englewood Cliffs, NJ, 1996.
- [5] B.-S. Kim, J. Li, and T.-C. Tsao, "Two-Parameter Robust Repetitive Control With Application to a Novel Dual-Stage Actuator for Noncircular Machining," *IEEE/ASME Transactions on Mechatronics*, vol. 9, pp. 644–652, Dec. 2004.
- [6] A. Sacks, M. Bodson, and W. Messner, "Advanced methods for repeatable runout compensation [disc drives]," *IEEE Transactions on Magnetics*, vol. 31, no. 2, pp. 1031–1036, 1995.
- [7] J. Zhang, S. Weerasooriya, T. Huang, and T. Low, "Modified AFC runout cancellation and its influence on trackfollowing," in *Industrial Electronics, Control and Instrumentation, 1997. IECON 97. 23rd International Conference on*, vol. 1, pp. 35–40, 1997.
- [8] J. Zhang, R. Chen, G. Guo, and T.-s. Low, "Modified adaptive feedforward runout compensation for dual-stage servo system," *IEEE Transactions on Magnetics*, vol. 36, no. 5, pp. 3581–3584, 2000.
- [9] W. Messner and M. Bodson, "Design of adaptive feedforward controllers using internal model equivalence," in *American Control Conference, 1994*, vol. 2, pp. 2–6, 1994.
- [10] L. L. Beranek and I. L. Ver, *Noise and Vibration Control Engineering, Principles and Applications*. New York: John Wiley & Sons, Inc, 1992.
- [11] G. F. Franklin, J. D. Powell, and M. Workman, *Digital Control of Dynamic Systems*. Ellis-Kagle Press, 3rd ed., 1998.
- [12] G. Welch and G. Bishop, "An introduction to the Kalman filter," *University of North Carolina at Chapel Hill, Chapel*, pp. 1–16, 1995.
- [13] R. Kalman, "A new approach to linear filtering and prediction problems," *ASME Journal of basic Engineering*, vol. 82, no. Series D, pp. 35–45, 1960.
- [14] J. Deyst and C. Price, "Conditions for asymptotic stability of the discrete minimum-variance linear estimator," *Automatic Control, IEEE Transactions on*, vol. 13, no. 6, pp. 702–705, 1968.
- [15] J. Doyle, "Gauranteed Margins for LQG Regulators," *IEEE Transactions on Automatic control*, vol. 23, pp. 756–757, Sept. 1978.
- [16] L. Brown and J. Schwaber, "Intermittent cancellation control: a control paradigm inspired by mammalian blood pressure control," *Proceedings of the 1999 American Control Conference (Cat. No. 99CH36251)*, no. June, pp. 139–143, 1999.
- [17] Y. Wang, K. Chu, and T.-c. Tsao, "Analysis and Control of Linear Motor for Nanopositioning," in *ASME Dynamic Systems and Control Conference*, (Hollywood, CA), 2009.
- [18] M. Athans and P. Falb, *Optimal Control*. New York: McGraw-Hill, 1966.

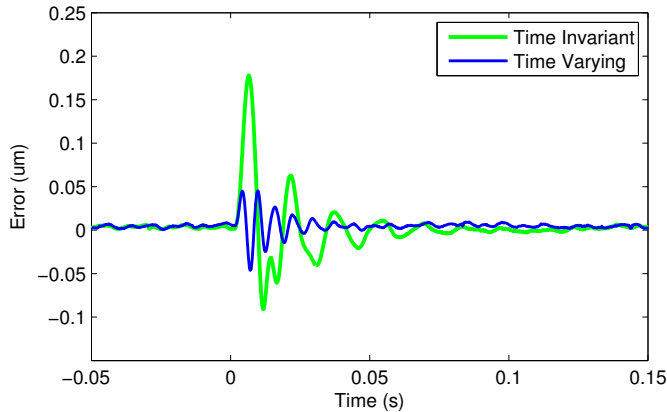


Fig. 13. Experiment: Output error performance due to an onset of sinusoidal disturbance

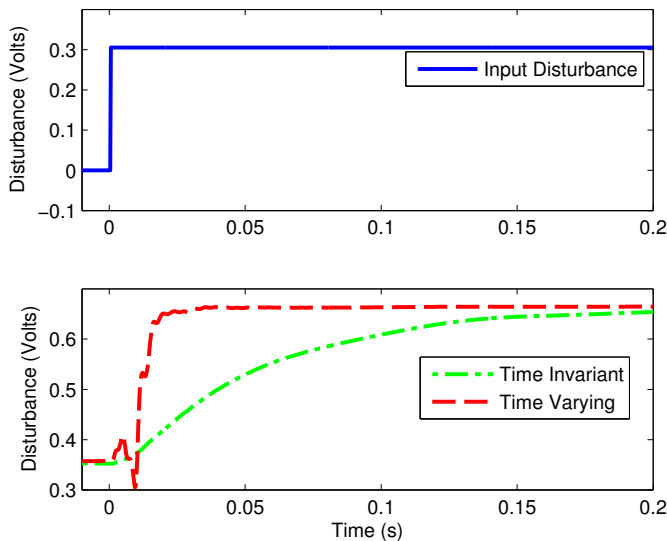


Fig. 14. Experiment: Disturbance estimation due to onset of constant disturbance.

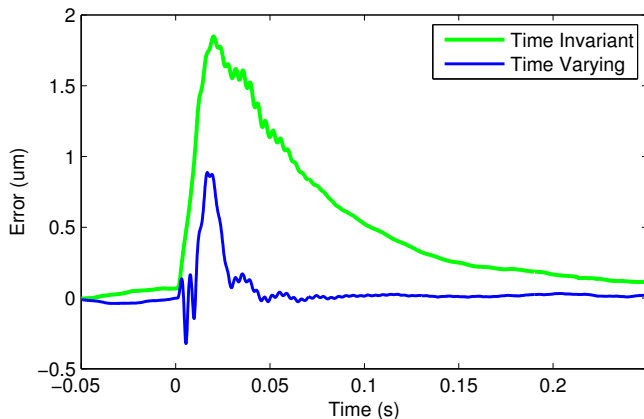


Fig. 15. Experiment: Output error performance due to onset of step disturbance at time zero